EPJ Web of Conferences **67**, 02112 (2014)
DOI: 10.1051/epjconf/20146702112

Numerical Simulation of Flow in Hub-Gap of Axial Stator Blades

Petr Straka[1,a]

[1] Aeronautical Research and Test Establishment, Beranových 130, 199 05 Prague-Letňany, Czech Republic

Abstract. In this paper there is described the numerical simulation of flow in the axial stator blade cascade with the radial gap between the hub and the stator blades. Influence of the gap size on distributions of the pressure, the Mach number, the kinetic energy losses, and the flow angle along the span is presented. There is also studied the possibility of modifying the shape of the hub to restrict the flow rate through the radial gap.

1 Introduction

The axial steam turbines of low power are typically designed with the drum-type rotor. For reduction of a production cost a seal-less stator wheels are still in use. In this configuration of the stator it is necessary to maintain the radial gap between the hub and the stator blades. However, flow through the radial gap generates large secondary flow structures which has negative influence on the efficiency. Influence of the secondary flow through the radial gap must be taken into account in the design of the blades. The available empirical informations (e.g. [1]) are often out of date or quite simplified. Therefore, research of the influence of the radial gap on flow in the axial turbine stages is still very actual. Currently, the numerical methods are gaining importance in research of the secondary flow in the turbine stages [2,3].

This paper deals with a numerical modelling of flow in the stator blades with the radial gap between the hub and the blades. Attention is paid to the influence of the radial gap on distribution of the Mach number, the pressure, the flow angle and the kinetic energy losses along the span. Also the mass flux ratio through the radial gap and the total losses of the kinetic energy are discussed. Subsequently it is studied change of the shape of the hub to reduce of the flow rate through the radial gap.

2 Simulation setup

Flow in axial stator is modeled as three-dimensional, steady, compressible, viscous, turbulent. The flowing medium is the perfect gas. The simulation is performed using the in-house numerical code based on solution of system of the RANS equation and the $k-\omega$ turbulence model. Used numerical code [4,5] is focused on turbomachinery application.

In figure 1 there is shown a scheme of the computational domain. The computational domain covers periodical section of stator wheel which contains one stator blade. At the inlet boundary the total pressure p_{01}, the total temperature $T_{01} = 300$ K, axial direction of the velocity vector, the turbulence intensity $Tu_1 = 3\%$ and a ratio of the turbulent to the molecular viscosity $\mu_t/\mu = 10$ are prescribed. At the outlet boundary the static pressure p_2 is prescribed. The walls are modeled as non-slip and adiabatic. Values of the total pressure p_{01} and the static pressure p_2 satisfies prescribed isentropic output Mach number $M_{2is} = 0.65$ and the isentropic output Reynolds number $Re_{2is} = 1.3 \times 10^5$. The outlet boundary condition is realized with respect to compliance with the radial equilibrium condition. Computation is performed for various size of the radial gap: 0.6 mm, 1.0 mm, 1.4 mm and for idealized case with zero gap.

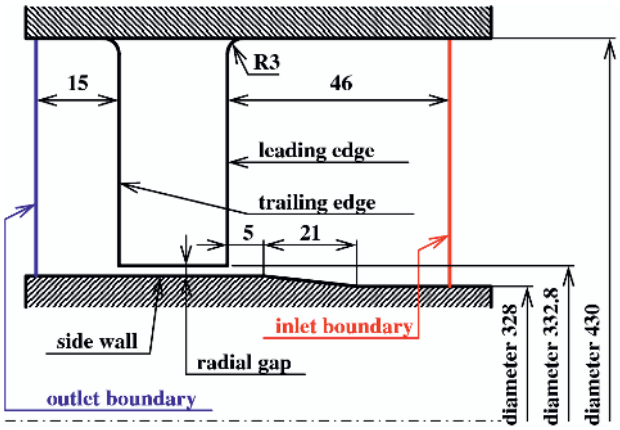

Fig. 1. Scheme of the computational domain (dimensions in millimeters).

3 Numerical results

In figures 3 to 6 there are shown spanwise distributions of the normalized outlet pressure, the outlet Mach number, the energy losses and the flow angles α and β (which are defined in figure 7). It is clear that the secondary flow influences from 15% to 25% of the span for gap size from 0.6 mm to 1.4 mm. In particular, deviation of the flow angle and increase of the kinetic energy losses near the hub are dramatic. In figure 8 there is shown the dependence of the total losses of the kinetic energy on the gap size. It is clear, that for gap 1.4 mm the losses are twice greater than in the idealized case without the radial gap. Figure 9 shows dependency of the total mass flux and the mass flux through

[a] e-mail: straka@vzlu.cz

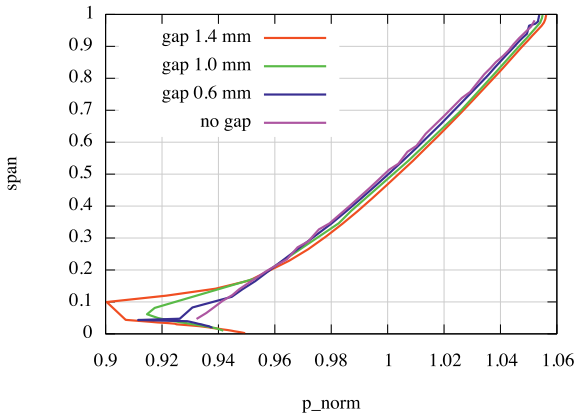

Fig. 2. Spanwise distribution of the normalized outlet pressure.

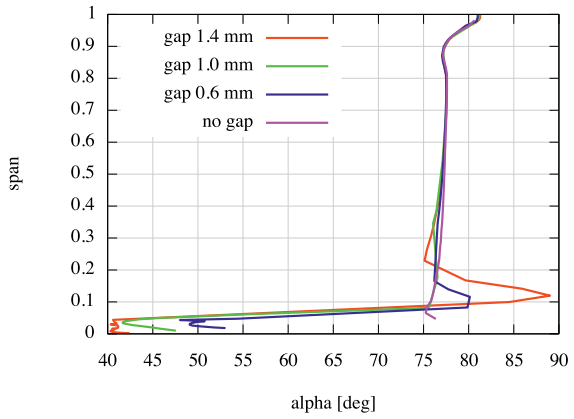

Fig. 5. Spanwise distribution of the flow angle α.

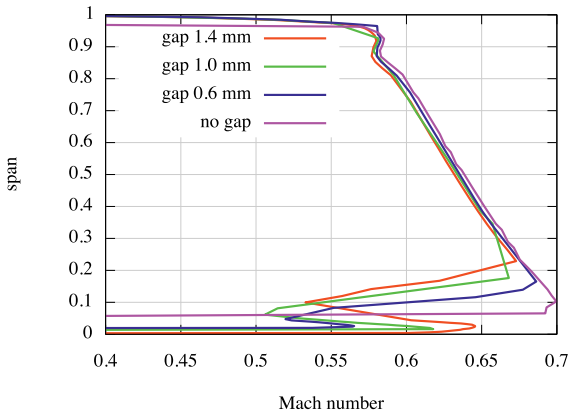

Fig. 3. Spanwise distribution of the outlet Mach number.

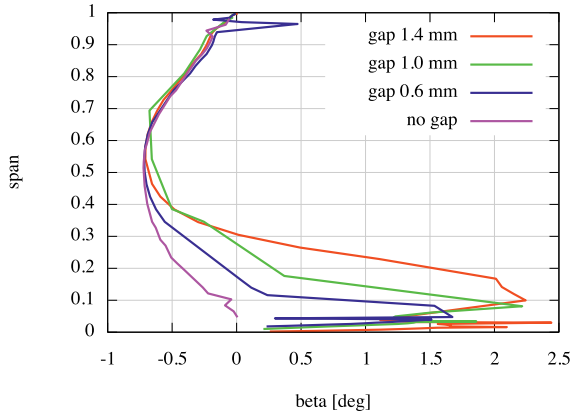

Fig. 6. Spanwise distribution of the flow angle β.

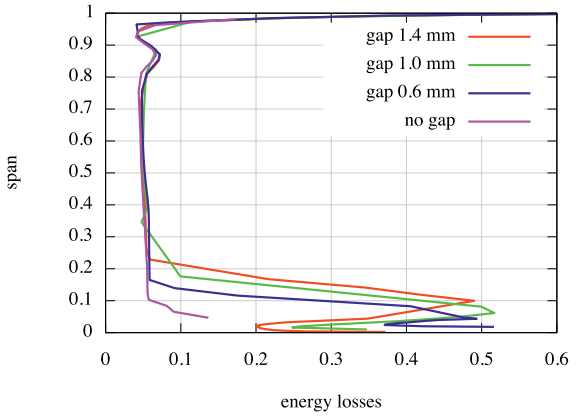

Fig. 4. Spanwise distribution of the energy losses.

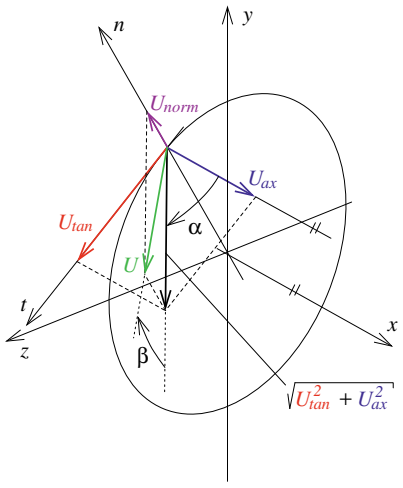

Fig. 7. Definition of the flow angles.

the radial gap. It is evident that the mass flux through the radial gap linearly depends on the gap size.

Figures 10 to 13 shows differences in the Mach number field for various size of the radial gap. The Mach number field clearly illustrates increase of deviation of the flow angle near the hub with increasing the size of the radial gap.

Figures 14 to 17, where the entropy isosurface are shown, illustrates development of the secondary flow vortices. While in the idealized case with zero radial gap only a channel vortices in hub and tip region are generated, in cases with the radial gap masiv vortices due to flow through the radial gap are formed. It is seen that with increasing the size of the radial gap these vortex structures stretches as far as twenty percent of the span.

Distributions of the kinetic energy losses in the outlet section of the stator wheel are shown in figures 18 to 21. It is evident that the profile losses, shown as a wakes in the middle part of the span, contribute a minority share to the total kinetic energy loss compare to the secondary flow losses.

Values of the total mass flux, the mass flux through the radial gap and the kinetic energy losses are listed in table 1.

Table 1. Mass flux and kinetic energy losses.

radial gap [mm]	Q [kg/s]	Q_{gap} [kg/s]	$100 \times \frac{Q_{gap}}{Q}$ [%]	kinetic energy losses [1]
0	3.1495	0	0	0.0619
0.6	3.2537	0.1632	5.02	0.1041
1.0	3.3387	0.2736	8.19	0.1193
1.4	3.4329	0.3798	11.06	0.1250

Table 2. Mass flux and kinetic energy losses – reshaped hub.

embedment depth [mm]	Q [kg/s]	Q_{gap} [kg/s]	$100 \times \frac{Q_{gap}}{Q}$ [%]	kinetic energy losses [1]
0	3.2537	0.1632	5.02	0.1041
2.2	3.3917	0.1468	4.33	0.1250
3.2	3.4789	0.1416	4.07	0.1265
4.2	3.6244	0.1409	3.98	0.1437

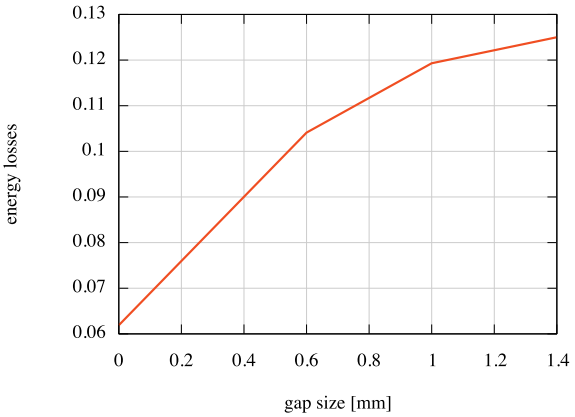

Fig. 8. Dependency of the total energy losses on gap size.

It is clear that with increasing the size of the radial gap increases total mass flux. This is caused by deflection of flow to the axial direction due to flow through the radial gap.

3.1 Reshaping hub

Previous results indicate a negative effect of the radial gap to conditions in the flow field. Considerable flow rate through the radial gap is given by high pressure difference on the pressure-side and the suction-side as shown in figure 22. The main idea of the hub reshaping is to change the pressure ratio on the pressure-side and the suction side near the radial gap and consequently reduce the flow rate through the radial gap. This should be achieved by embedding of the end of the blades into the hub as illustrated in figures 23 and 24.

Unfortunately, this modification, contrary to the assumption, does not improved the pressure ratio on the pressure-side and the suction-side as documented figure 25. Also distribution of the kinetic energy losses in figure 26 demonstrates, that embedding the end of the blades into the hub

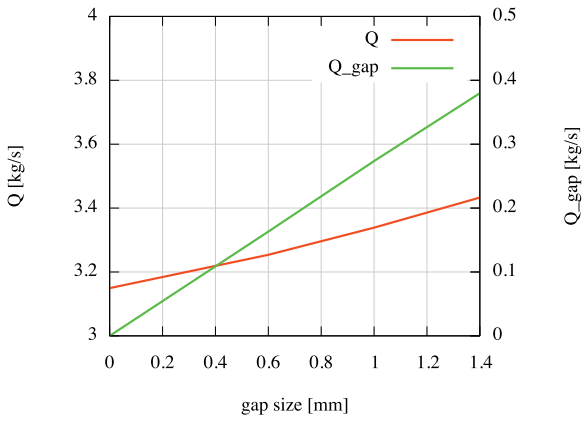

Fig. 9. Dependency of the total mass flux and mass flux through the radial gap on gap size.

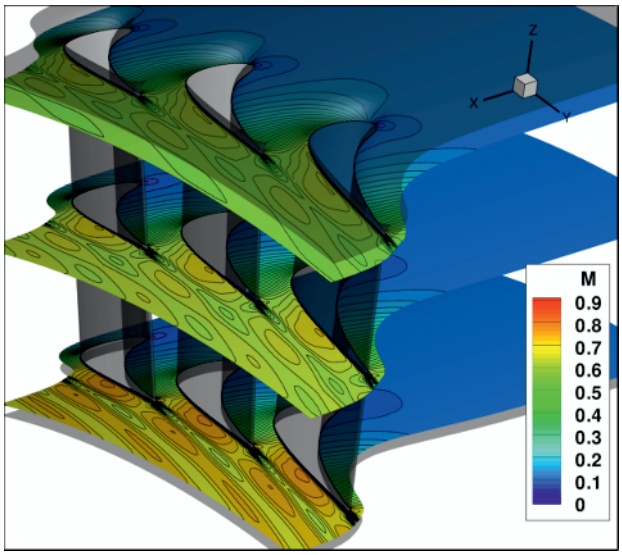

Fig. 10. Mach number field – zero gap.

does not leads to the improvement but to the deterioration of condition in the flow field. Values of the total mass flux, the mass flux through the radial gap and the kinetic energy losses for reshaped hub with various embedment depth are listed in table 2.

4 Conclusion

This study shows that the secondary flow through the radial gap strongly affects approximately twenty percent of the span. As a result of flow through the radial gap occurs a deflection of flow near the hub to the axial direction, which leads to increasing of total mass flux. The massive secondary vortices cause an increase in the kinetic energy losses almost up to twice compared with the idealized case without the radial gap. The tested method of modifying the shape of the hub does not improve conditions in the flow field near the hub. Contrary to the assumptions, embedding of the end of the blade into the hub, does not leads to limitation of the vortex structure at the outlet of the radial gap. Due to the shape of the hub, the vortex structure at the outlet of the radial gap rises up and affects a larger area of flow field compared to the case without reshaping of the

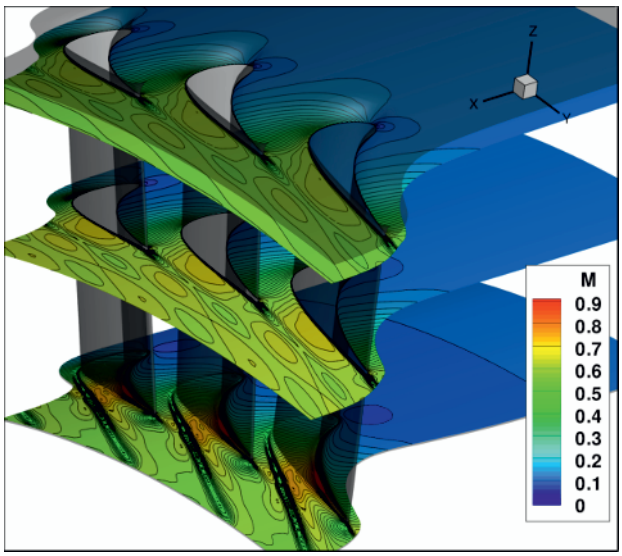

Fig. 11. Mach number field – gap size 0.6 mm.

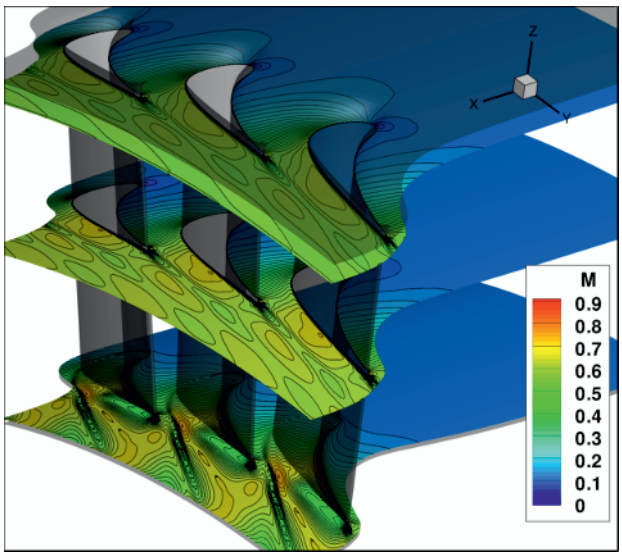

Fig. 12. Mach number field – gap size 1.0 mm.

hub. This leads to increase of the loss and to the deterioration of conditions near the hub.

Follow-up work will be test the possibility of change the shape of the hub-profile of the stator blade in order to improve the pressure ratio on the pressure-side and the siction-side near the hub and eliminate the disadvantage of prismatic blades.

5 Acknowledgement

This work was supported by the grant project TA02021336 of the Technology Agency of the Czech Republic.

References

1. V.A. Chernikov, Aerodyn. Characteristics of Therm. Turb. Stages, Leningrad, (1980) (in Russian)
2. MSc Thesis, MTI, Massachusetts, (2011)
3. T.C. Booth, VKI Lecture Series 1985-05, VKI, (1985)
4. P. Straka, Proc. Conf. Exp. Fluid Mech. 979-987, (2011)
5. P. Straka, Technical Report VZLÚ R-4910, Prague, (2010) (in Czech)

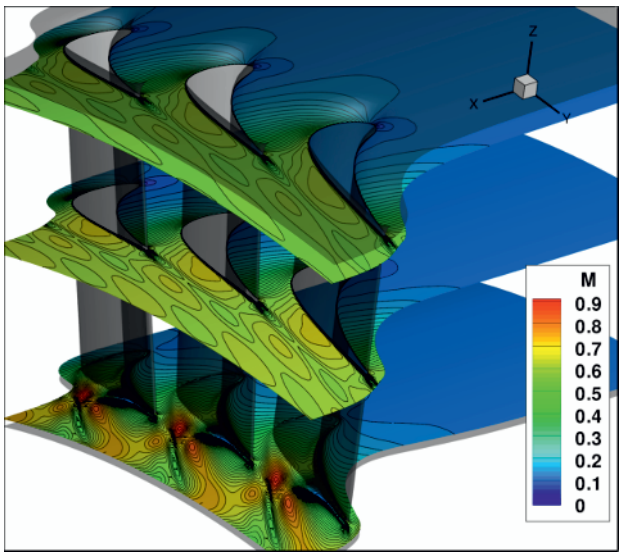

Fig. 13. Mach number field – gap size 1.4 mm.

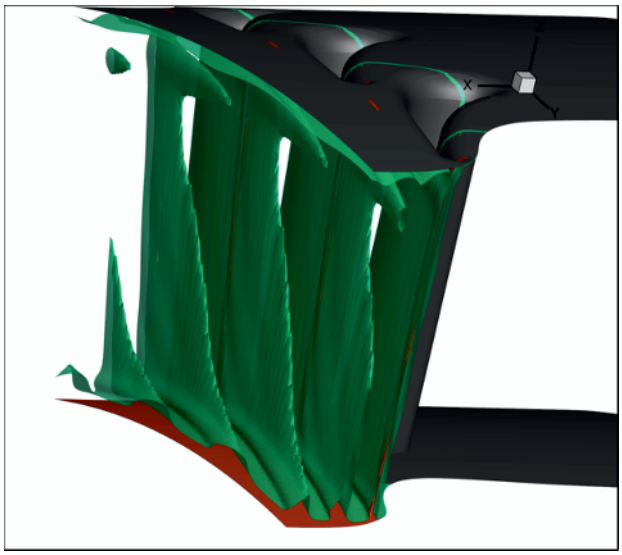

Fig. 14. Entropy isosurface – zero gap.

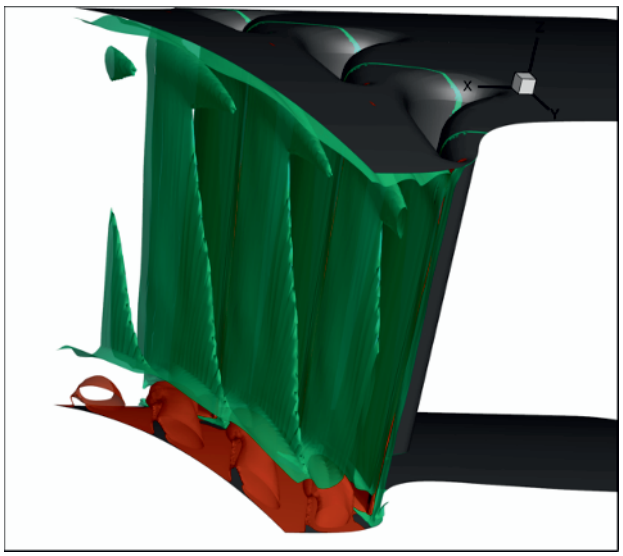

Fig. 15. Entropy isosurface – gap size 0.6 mm.

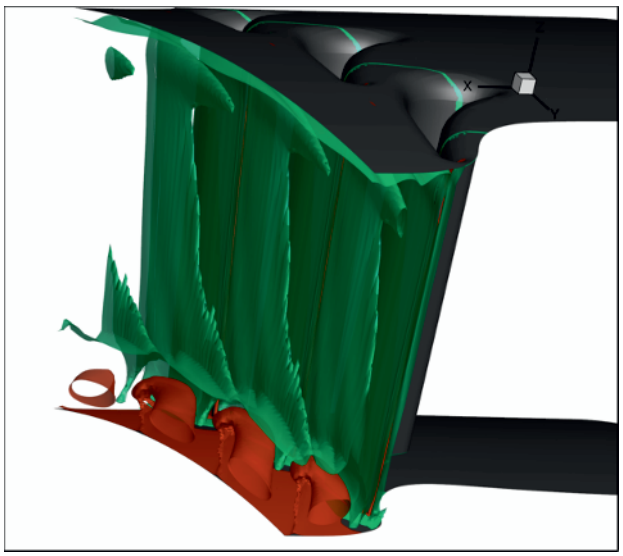

Fig. 16. Entropy isosurface – gap size 1.0 mm.

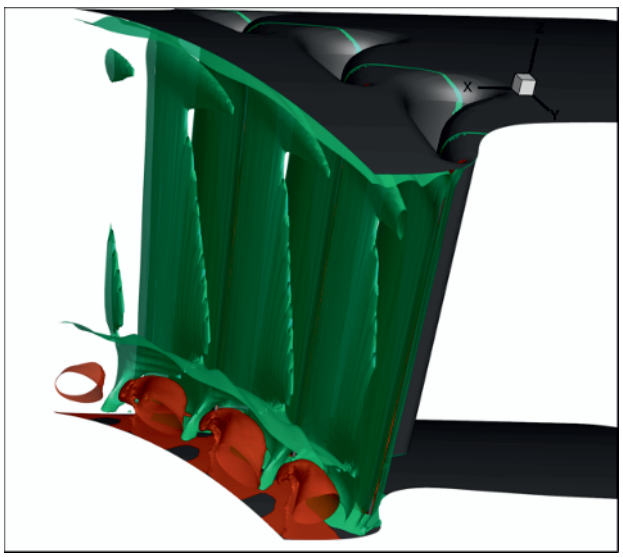

Fig. 17. Entropy isosurface – gap size 1.4 mm.

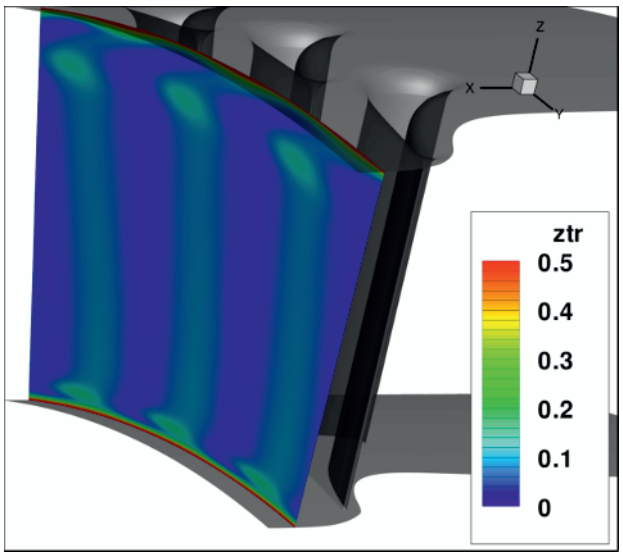

Fig. 18. Kinetic energy losses – zero gap.

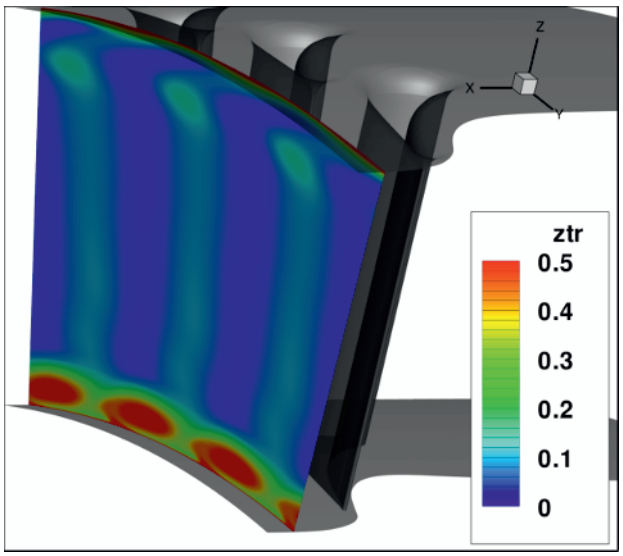

Fig. 19. Kinetic energy losses – gap size 0.6 mm.

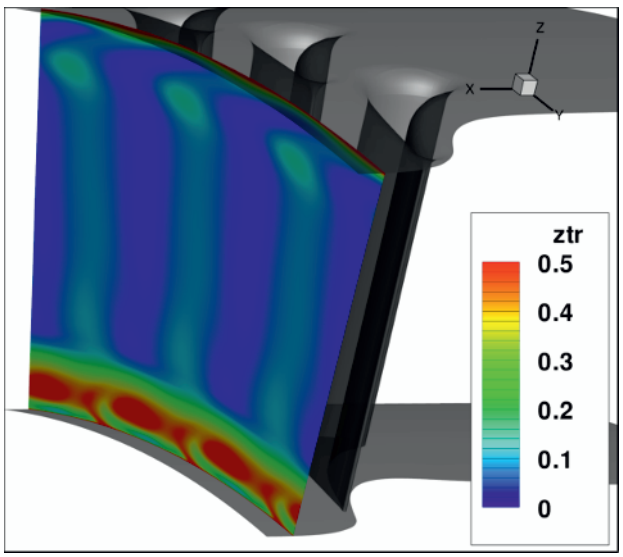

Fig. 20. Kinetic energy losses – gap size 1.0 mm.

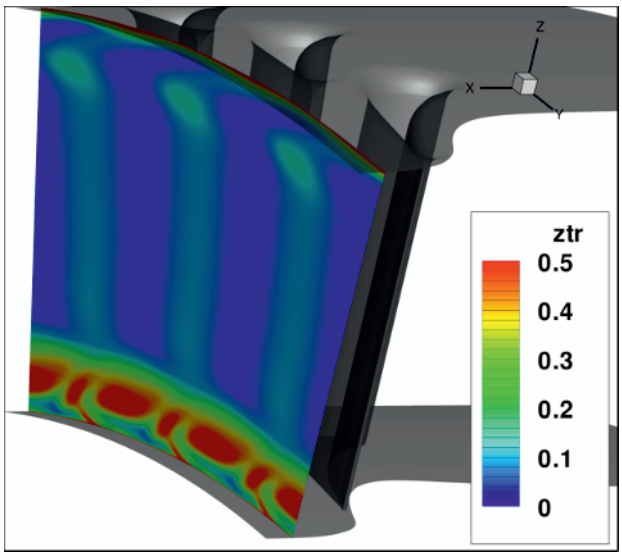

Fig. 21. Kinetic energy losses – gap size 1.4 mm.

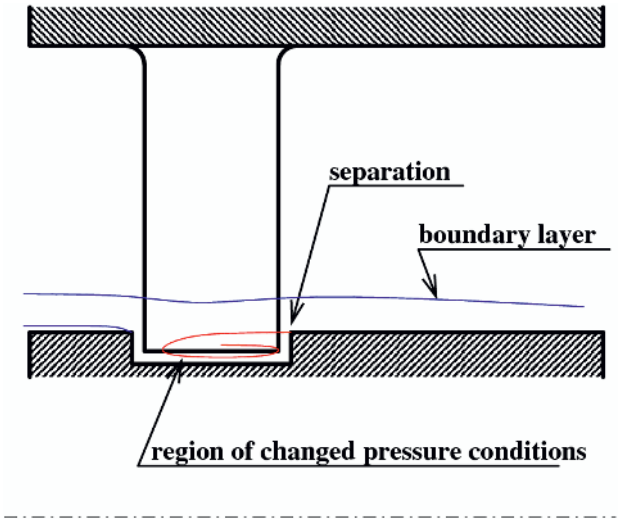

Fig. 24. Scheme of the computational domain with embedment of the end of the blade into the gap.

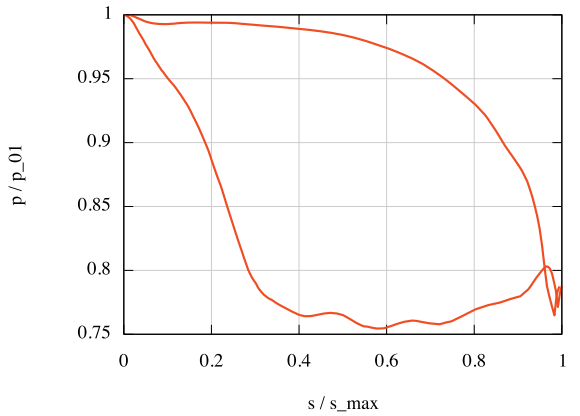

Fig. 22. Distribution of normalized pressure along the blade surface near the radial gap.

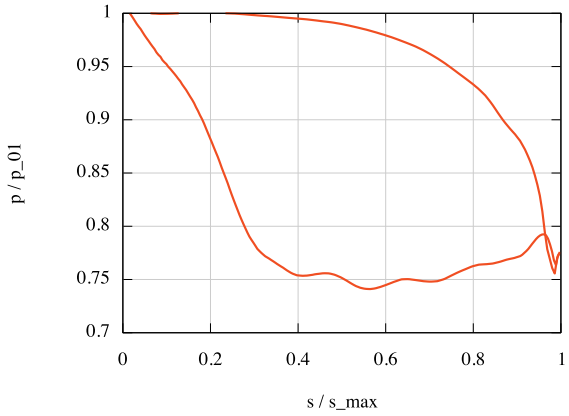

Fig. 25. Distribution of normalized pressure along the blade surface near the radial gap – reshaped hub.

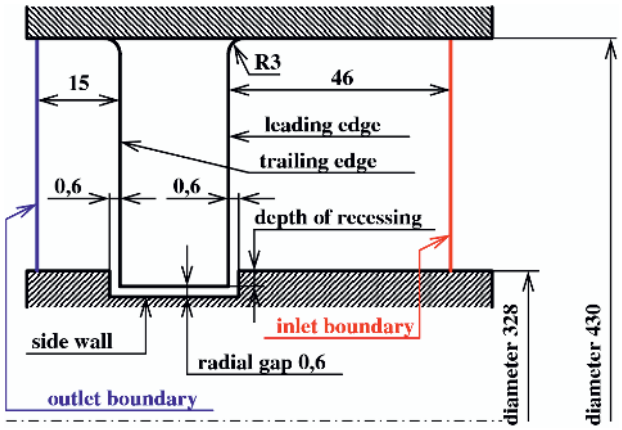

Fig. 23. Scheme of the computational domain with embedment of the end of the blade into the gap.

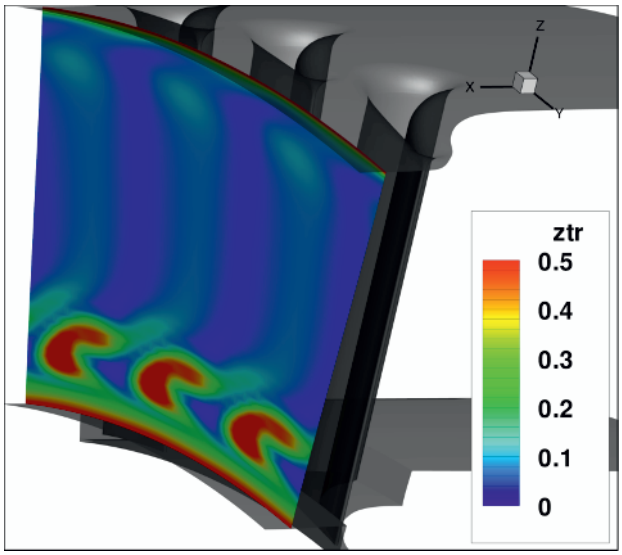

Fig. 26. Kinetic energy losses – reshaped hub.